

# Neural network model of creep strength of austenitic stainless steels

T. Sourmail, H. K. D. H. Bhadeshia, and D. J. C. MacKay

The creep rupture life and rupture strength of austenitic stainless steels have been expressed as functions of chemical composition, test conditions, stabilisation ratio, and solution treatment temperature. The method involved a neural network analysis of a vast and general database assembled from published data. The outputs of the model have been assessed against known metallurgical trends and other empirical modelling approaches. The models created are shown to capture important trends and to extrapolate better than conventional techniques. MST/5124

Dr Sourmail (ts228@cus.cam.uk) and Professor Bhadeshia are in the Department of Materials Science and Metallurgy, University of Cambridge, Pembroke Street, Cambridge CB2 3QZ, UK and Dr MacKay is in the Department of Physics, Cavendish Laboratory, University of Cambridge. Manuscript received 12 June 2001; accepted 4 September 2001.  
© 2002 IoM Communications Ltd.

## Introduction

Austenitic stainless steels are commonly used in the power generation industry at temperatures greater than 650°C and stresses of 50 MPa or more, and are expected to remain in service for more than 100,000 h. Such time periods are seldom accessible experimentally and long-term properties are often extrapolated from shorter term tests conducted at high stresses. Therefore great care is needed in extrapolating the experimental data during design. A further difficulty in trying to predict the long term properties of austenitic steels is the strong influence of alloying elements and their numerous interactions. This explains why most of the empirical approaches are restricted to limited ranges of compositions, for example, equation (1) has been proposed for the  $10^4$  h creep rupture stress ( $\sigma_{r,10^4}$ ) of a AISI 316 at 650°C

$$\sigma_{r,10^4} = 173 \cdot 8 + 7243[B] + 961 \cdot 1[N] + 1145[S] - 7 \cdot 5[Cr] \quad (1)$$

while equation (2) is for a 304 steel at the same temperature<sup>1</sup>

$$\sigma_{r,10^4} = 90 \cdot 81 + 115[Mo] + 498 \cdot 5[W] \dots \dots \dots (2)$$

where the concentrations are in wt-%. The range for each variable is not given in Ref. 1, but it appears that equation (2) does not even cover the range of composition that separates an AISI 304 steel from an AISI 316.

Such equations often come from limited studies and therefore only address the role of a few alloying elements. As a consequence of the restricted amount of data on which they are based, these equations seldom account for interactions between variables. Finally, they do not account explicitly for the effects of temperature, time, and stress.

Neural networks represent a more general regression method, which ameliorates most of the problems encountered with linear regression. In the present study, neural network analysis was applied to a database covering a vast range of compositions of austenitic stainless steels to estimate the creep rupture life and the creep rupture stress as a function of many parameters.

## Method

A neural network is a parameterised non-linear model which can be used to perform regression, in which case, a very flexible, non-linear function is fitted to experimental data. the details of this method have been reviewed

elsewhere,<sup>2,3</sup> but it is nevertheless useful to introduce its main features.

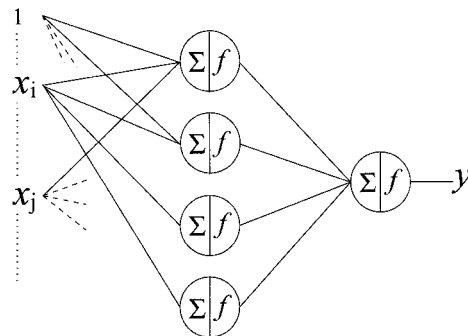
Simple three layer feedforward networks are used, such as the one shown in Fig. 1. The activation function for the neurons in the second layer (equation (3)) is tanh while it is linear (equation (4)) in the third one

$$h_i = \tanh \left( \sum_j w_{ij}^{(1)} x_j + \theta_i^{(1)} \right) \dots \dots \dots (3)$$

$$y = \sum_i w_i^{(2)} h_i + \theta^{(2)} \dots \dots \dots (4)$$

$x_i$  are the inputs and  $w_i$  the parameters, or weights, which define the network. The biases  $\theta_i$  are treated internally as weights associated with a constant input set to unity. Any non-linear function can be used at the hidden units (as long as it is continuous and differentiable), and tanh is a standard choice for such networks. A linear function for the output is a simple choice to ensure that all values can be taken (tanh would limit the output to  $\pm 1$ , for example).

The complexity of such models scales with the number of neurons in the second layer, most often referred to as the hidden units. The neural network can capture interactions between the inputs because of the non-linearity of the activation function. The nature of these interactions is implicit in the weights but they are often difficult to interpret directly. The best way to identify the interactions is to use the network to make predictions and see how these depend on various combinations of input.



1 Three layer feedforward network similar to that used in this work: activation function of the neurons in second layer is a tanh, and is linear in the third one; the models complexity is controlled by number of neurons in the second layer, also called hidden units

Many training methods involve finding the weights which minimise an objective function, typically

$$\left. \begin{aligned} M(w) &= \beta E_D + \alpha E_W \\ E_D &= \frac{1}{2} \sum_i (t^{(i)} - y^{(i)})^2 \\ E_W &= \frac{1}{2} \sum_i w_i^2 \end{aligned} \right\} \dots \dots \dots (5)$$

where  $E_D$  is the overall error, and  $E_W$  the regulariser, used to force the network to use small weights (equations (5));  $\alpha$  and  $\beta$  are control parameters which largely influence the complexity of the model;  $t^{(i)}$  is the target for the set of inputs  $\mathbf{x}^{(i)}$ , while  $y^{(i)}$  is the corresponding network output.

The method used in this study, developed by MacKay,<sup>4</sup> is based on Bayesian probability theory and treats learning as an inference problem.

Rather than trying to identify the best set of weights, the algorithm infers a probability distribution for the weights from the data presented. When making predictions, the variety of solutions corresponding to different possible sets of weights are averaged using the probabilities of these sets of weights, a process called marginalising.

A major consequence is that it is possible to quantify the uncertainty of fitting: if the inferred distribution is sharply peaked in the weight space, the most probable set will give by far the largest contribution to the prediction and alternative solutions will have little importance. As a consequence, the prediction will be associated with a small uncertainty. If, on the contrary, the data are such that different sets of weights are similarly probable, alternatives will contribute in similar proportions and the error bar will be large, as typically occurs in regions of the input space where data are scarce or exceptionally noisy.

In this context, the performances of different models are best evaluated using the log predictive error (LPE) as defined below. This error penalises wild predictions to a lesser extent when they are accompanied by appropriately large error bars

$$\text{LPE} = \sum_m \left[ \frac{1}{2} (t^{(m)} - y^{(m)})^2 / \sigma_y^{(m)^2} + \log(2^{1/2} \pi^{1/2} \sigma_y^{(m)}) \right] \quad (6)$$

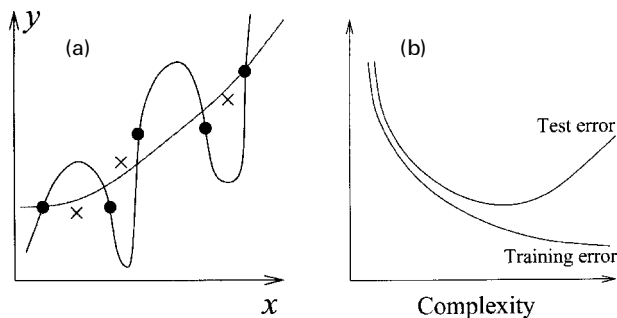
where  $\sigma_y^{(m)}$  is related to the uncertainty of fitting for the set of inputs  $\mathbf{x}^{(m)}$ .

## OVERFITTING PROBLEM

Because of the great flexibility of the functions used in the network, there is a possibility of overfitting data. Two solutions are implemented which contribute to avoid overfitting. The first is contained in the algorithm due to MacKay:<sup>4</sup> the complexity parameters  $\alpha$  and  $\beta$  are inferred from the data, therefore allowing automatic control of the model complexity.

The second resides in the training method. The database is equally divided into a training set and a testing set. To build a model, about 150 networks are trained with different numbers of hidden units and seeds, using the training set; they are then used to make predictions on the unseen testing set and are ranked by LPE. Figure 2 illustrates the behaviour of the error on the training and the testing set. Because it is possible to obtain a near perfect fitting, the error on the training set is always decreasing with increasing complexity. The error on the testing set decreases at first, as the fitting improves, but increases again when overfitting occurs.

To ensure a good distribution of the data in the two subsets, the database is initially randomised. The input and outputs are then rescaled into the interval  $\pm 0.5$ , this step is not obligatory but is a convenient way of comparing the effect of different variables on the output.



2 a when a model has overfitted the training data ●, the error on test data × is larger than for an optimum model which fits the trend but not the noise; b behaviour of error on training and testing sets as function of complexity of the model is illustrated

## COMMITTEE MODEL

As is evident from the above discussion, networks with different numbers of hidden units will give different predictions. But predictions will also depend on the initial guess made for the probability distribution of the weights (the prior).

Optimum predictions are often made using more than one model, by building a committee. The prediction  $\bar{y}$  of a committee of networks is the average prediction of its members, and the associated error bar is calculated according to

$$\left. \begin{aligned} \bar{y} &= \frac{1}{L} \sum_l y^{(l)} \\ \sigma^2 &= \frac{1}{L} \sum_l \sigma_y^{(l)^2} + \frac{1}{L} \sum_l (y^{(l)} - \bar{y})^2 \end{aligned} \right\} \dots \dots \dots (7)$$

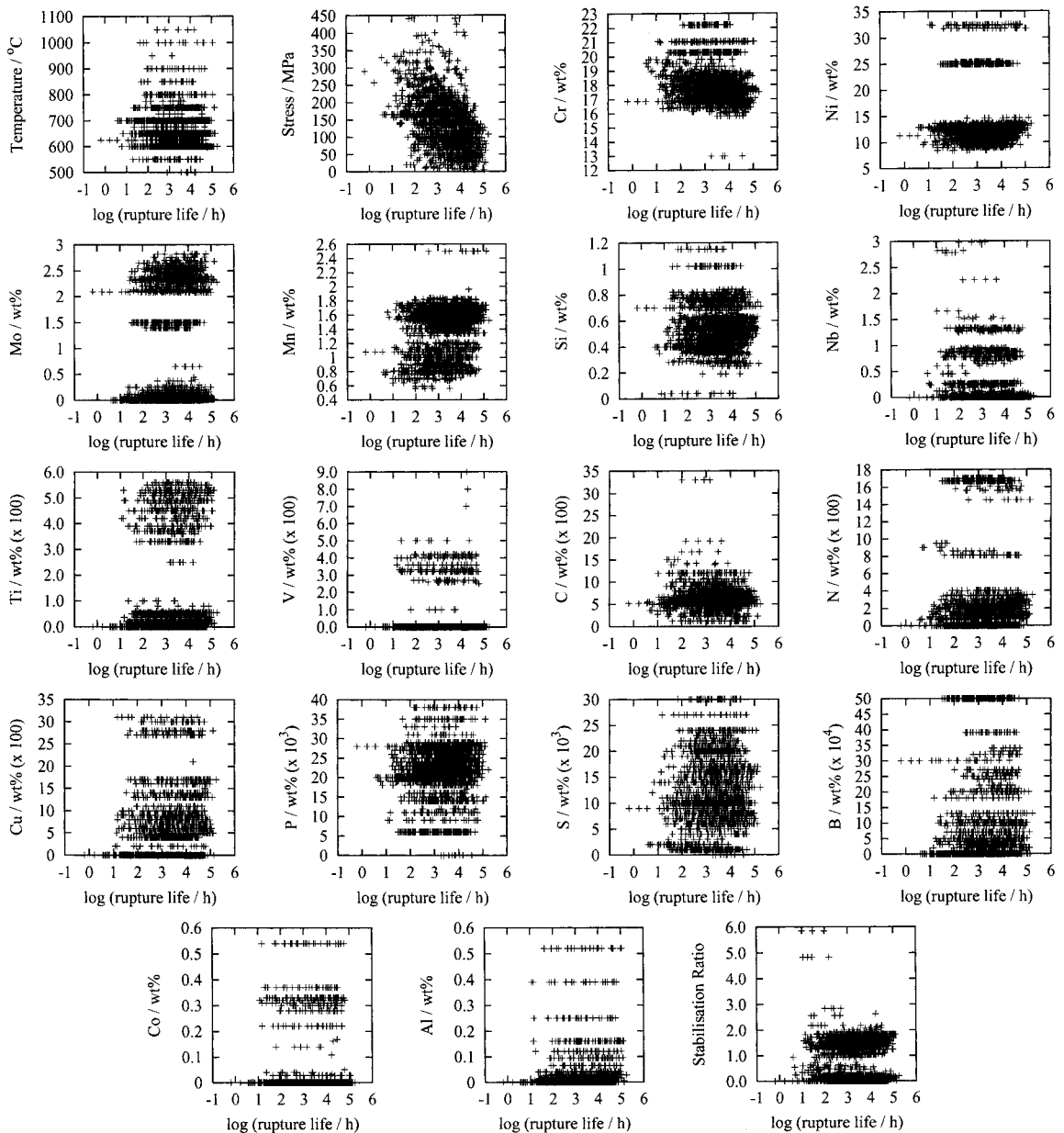
where  $L$  is the number of networks in the committee. Note that we now consider the predictions for a given, single set of inputs and that the exponent  $l$  refers to the model used to produce the corresponding prediction  $y^{(l)}$ . In practice, an increasing number of networks are included in a committee and their performances are compared on the testing set. Most often, the error is minimum when the committee contains more than one model. The selected models are then retrained on the full database.

## Database

A large database was compiled for the creep properties of various grades of austenitic stainless steels: AISI 304 (basic 18Cr–12Ni), AISI 316 (304+ Mo), AISI 321 (304+ Ti), AISI 347 (304+ Nb) and many variants designed for heat resistant applications (for example, 316+ Ti, Esshete 1250, etc.). It contains a total of about 3500 entries which, as explained above, are equally distributed between the training and testing sets. Figure 3 gives an idea of the distribution of each input against the logarithm of the rupture life.

The dataset included all of the following NIRM (National Research Institute for Metals, Japan) datasheets: 5B, 6B, 45, 28A, 16B, 26B, 14B, and most of the data published by the British Steelmakers Creep Committee<sup>5</sup> for 304, 316, 321, and 347. Only limited data could be extracted from publications.<sup>6–21</sup> This is essentially because of non-standard pretest mechanical treatments performed in order to accelerate the evolution of the microstructure.

The data set includes the following variables: test conditions (stress and temperature), chemical composition, solution treatment temperature and time (the latter being available in a very limited number of cases), nature of the quench following, grain size, and logarithm of ruptured life. The minimum and maximum values are given in Table 1.



3 Distribution of the different inputs v. log of creep rupture life: this way of representing the data should not hide the possibility of numerous non-documented interactions

Because the algorithm includes an automatic relevance detection,<sup>22</sup> variables which are either redundant or found to be irrelevant are accorded a zero weight. There is therefore little to gain in reducing the number of input variables by any other process.

Compositional data were often missing. In such circumstances, elements usually known to be deliberate additions were set to zero while impurities were set to the average of the available data (e.g. phosphorus and sulphur). There is undoubtedly a regrettable loss of information when the amounts of elements such as Mo or Nb present as impurities are not given, as there is evidence that these elements have an influence.<sup>1</sup>

## Creep rupture life model

It is usual to attempt to predict the rupture strength for a given lifetime. However, the creep stress is only present as a finite number of discrete values while the rupture life is

much more continuously spread, and therefore seemed a more appropriate target.

When training a model, the choice of input variables is of great importance. Also, when a combination of these variables is believed to be of particular importance, the model can be improved by adding the combination as an explicit variable. The model was trained on the logarithm of the rupture life rather than the rupture life itself, and the calculated stabilisation ratio was used, as given below

$$\text{stabilisation ratio} = \frac{[\text{Nb}]/8 + [\text{Ti}]/4}{[\text{C}] + [\text{N}]} \quad (8)$$

where the concentrations are in wt-%. This is because precipitation of MX (where M is either Nb or Ti and X either C or N) is believed to be of particular importance to the creep behaviour of austenitic stainless steels, as will be discussed in more detail below. To avoid biasing the model, the individual variables making up the stabilisation ratio are also included, so that a direct influence of any of them can also be detected. Other input variables are as given in Table 1.

Because some inputs were not always given (the solution treatment temperature for example), about 1000 among the 3500 entries of the database could not be used. About 130 networks were trained with up to 22 hidden units and 6 different seeds. As expected, the perceived level of noise during training decreases as the model becomes more complex. The results of the training are shown in Fig. 4.

The purpose and method for building a committee model has been discussed above. In this case, the optimum committee was found to have four members. The perceived significances  $\sigma_w$  for these four models are shown in Fig. 5. They represent the extent to which a particular input explains the variation of the output, rather like a partial correlation coefficient in a multiple linear regression analysis.

The predictions of the final committee model (Fig. 6) contain very few outliers considering that there is a total of about 2000 points. The improvement is clear compared with the best model alone.

## Creep strength model

The creep strength model was built essentially to facilitate quantitative comparisons with the literature. In this case, the target was the stress and the life time was an input. The solution treatment temperature was not included to allow use of the entire database.

It seems of little interest to reproduce here all the results from the training such as test error or LPE as a function of number of hidden units as their evolution was similar to that observed for the creep rupture life model. In this case, the optimum number of models in committee was found to be 12. The performance of the best model is shown in Fig. 7 and that of the committee in Fig. 6.

## Applications

### MOLYBDENUM IN AISI 304 AND AISI 316

The difference between AISI grades 304 and 316 resides essentially in the addition of about 2 wt-% of molybdenum. The chromium and nickel concentrations are smaller and larger, respectively, for AISI 316 compared with AISI 304.

Table 1 Various inputs in data set

Input variable	Min.	Max.	Mean	Standard deviation
Test stress, MPa	5	443	145	72
Test temperature, °C	500	1050	667	71
Log (rupture life, h)	-0.200	5.240	3.324	0.879
Composition, wt-%				
Cr	12.98	22.22	18.08	1.35
Ni	8.40	32.48	13.82	5.47
Mo	0.00	2.82	1.05	1.10
Mn	0.56	2.50	1.36	0.35
Si	0.040	1.150	0.545	0.171
Nb	0.000	2.980	0.242	0.449
Ti	0.000	0.560	0.131	0.199
V	0.000	0.090	0.004	0.011
Cu	0.000	0.310	0.051	0.074
N	0.000	0.170	0.029	0.052
C	0.012	0.330	0.062	0.025
B	0.000	0.005	0.001	0.0016
P	0.000	0.038	0.021	0.0067
S	0.000	0.030	0.012	0.0071
Co	0.000	0.540	0.037	0.1090
Al	0.000	0.520	0.029	0.0804
Solution treatment temperature (°C)	1000	1350	1102	51

Rupture stresses for  $10^4$  h at  $650^\circ\text{C}$  are respectively around 80 MPa and 110 MPa.<sup>23</sup>

There are no specifications as to what the maximum level of Mo should be for the AISI 304 steels. It is common to find up to 0.5 wt-%Mo in these steels. For AISI 316, an addition of 2–3 wt-%Mo is specified. It has been shown that Mo has a beneficial effect on creep strength because of its solution strengthening role, although this effect can disappear after prolonged aging owing to the formation of a Mo rich Laves phase.<sup>1</sup>

Figure 8 illustrates the predicted effect of Mo on the  $10^4$  h rupture stress. The initial increase is consistent with equation (2), which predicts a strong effect of small additions of Mo in 304. The predicted gradient (assuming a linear variation) is 38 MPa per wt-% between 0 and 0.02 wt-%Mo, which is lower than the one given by equation (2). Particularly interesting is that the trend between 0 and 1.1 wt-% of Mo shows an excellent agreement (correlation 0.995) with a  $c^{1/2}$  (where  $c$  is the concentration) dependence expected for a solution strengthening mechanism.<sup>24</sup>

The flattening of the curve would be consistent with precipitation of a Mo rich phase, which would keep the matrix content at a constant level. In this regard, the shift of the plateau between the  $10^4$  h and the  $10^5$  h rupture stress could be related to the kinetics of this precipitation. Calculations made on this composition with MT-DATA (Fig. 8B) actually reveal a consistent trend in the Mo content of the austenite when increasing the bulk Mo content, but indicate that Laves phase is only expected for a Mo content greater than 2.2 wt-%.

## CHROMIUM AND BORON

According to equation (1), chromium slightly reduces the creep rupture strength. Unfortunately the mechanism does not seem to be understood. It was possible to reproduce this trend for a type 316 steel as illustrated in Fig. 9. The gradient for compositions close to 16 wt-%Cr is in very good agreement with the value of 7.5 found in equation (1).

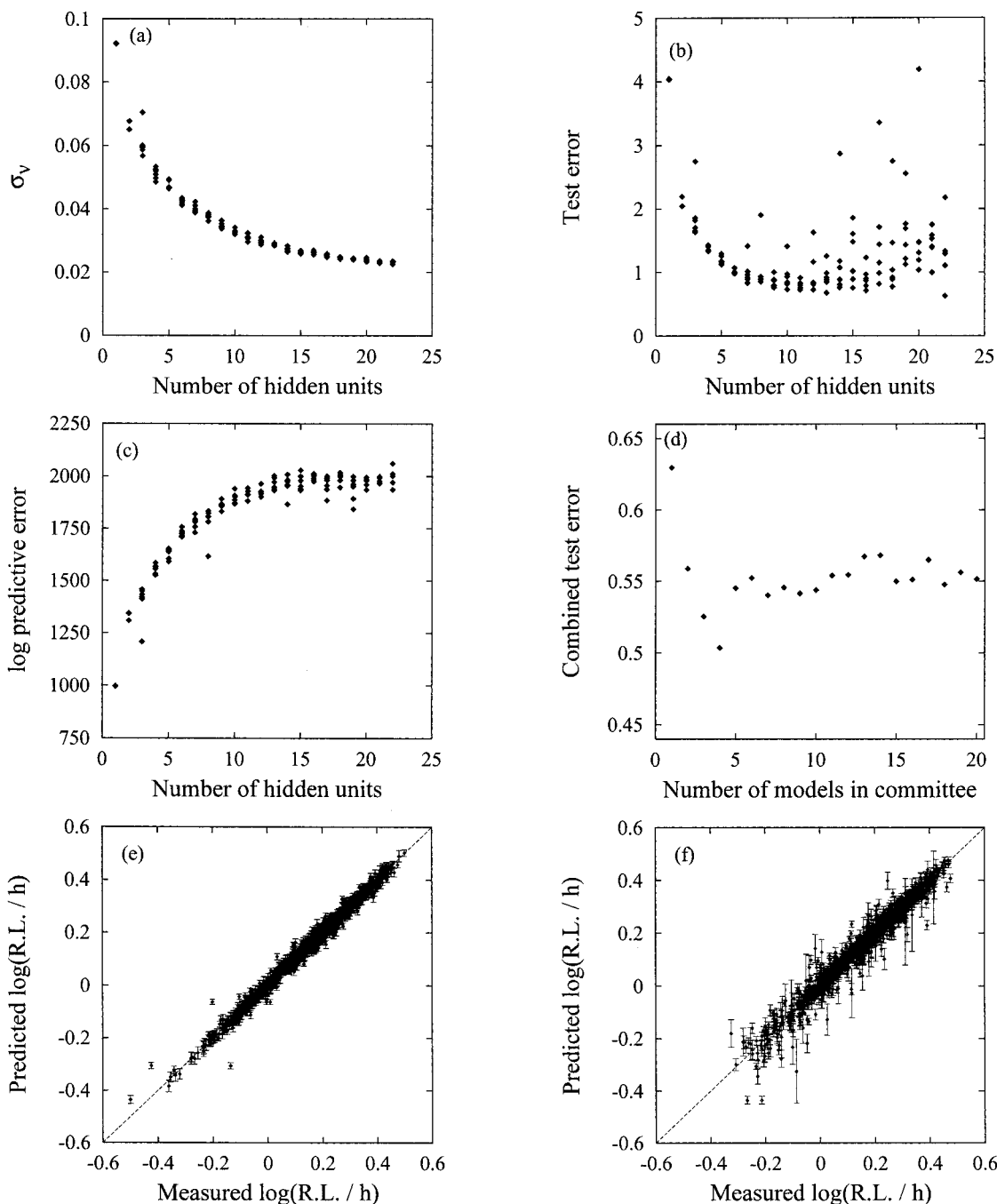
Additions of boron have been found to increase substantially the creep life of austenitic stainless steels, as emphasised by the large coefficient it is attributed in equation (1). The predicted effect of boron was found to be similar, with a slope of  $\sim 5700$  MPa per wt-% (see Fig. 9).

## STABILISATION RATIO AND SOLUTION TEMPERATURE

There has been much work on the influence of the amount of 'stabilising elements' such as Nb, Ti, V, or Zr, which prevent the formation of chromium carbides, on the creep properties of austenitic stainless steels. The problem is generally described using a stabilisation ratio (equation (8)), which is a convenient estimate of the extent to which carbon, nitrogen, and the stabilising elements deviate from stoichiometry during compound formation.<sup>10,25,26</sup>

Keown and Pickering<sup>13</sup> estimated that the best creep properties were obtained for stoichiometric additions of Nb while more recent work<sup>27</sup> claims that 'under stabilising' carbon and carbon kept in solution are better. This is because data from long term experiments<sup>27</sup> have shown that the trend observed by Keown and Pickering for rather short term experiments (average 3000 h) do not extrapolate well. For Ti on its own, the agreement is that a larger stabilisation ratio produces the optimum creep strength.<sup>1</sup>

For short term tests, optimum creep properties have often been found when the precipitation of MX was maximised by using stabilisation equal to or greater than unity. However, according to Ref. 1, the creep of austenitic steels is essentially diffusion controlled in service conditions, which

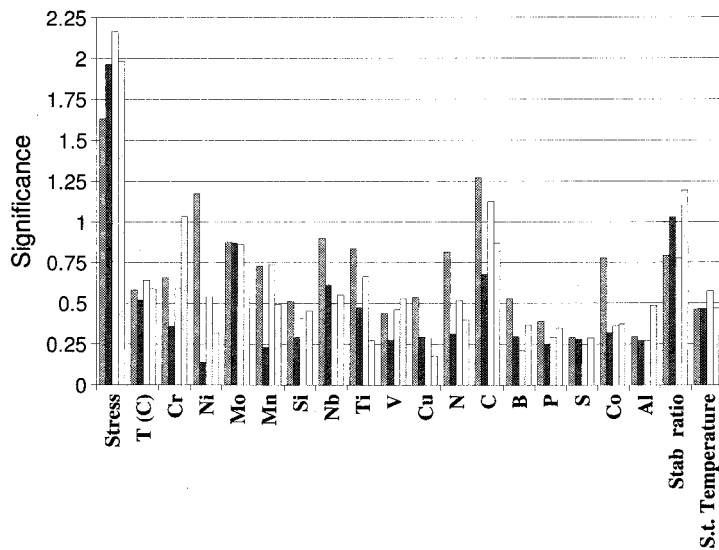


4 a perceived level of noise  $\sigma_v$ , b test error, c log predictive error of the models with increasing numbers of hidden units, the combined test error d for an increasing number of models in committee, and the performances of the best single model on seen (training set e) and unseen data (testing set f): e and f are plots of predicted rupture life (R.L.) against the experimental values, in this case both are normalised

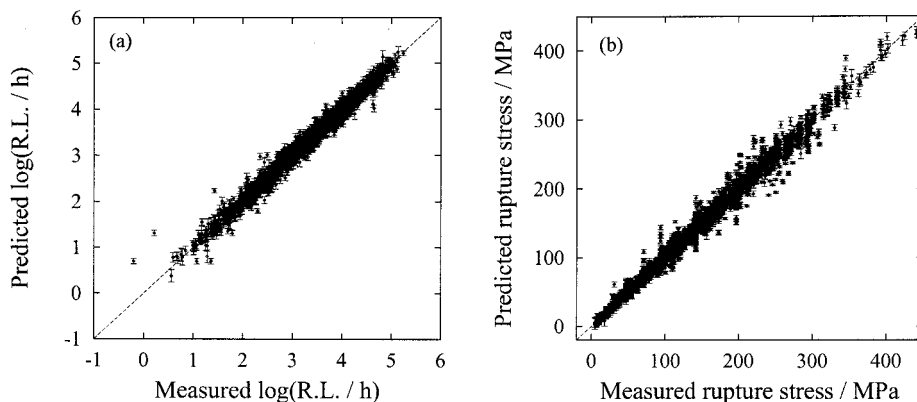
could explain why there is no great benefit in maximising the amount of MX precipitates.

Figure 10a, shows that the neural network model was able to reproduce the expected trends for Nb additions. For short term tests, the best properties are obtained for a stabilisation ratio equal to or slightly greater than unity. For longer term tests, the influence of stabilising elements is predicted to be less and the optimum addition much below a stoichiometric ratio. On the right of Fig. 10 is the effect of Ti addition on the  $10^4$  and  $10^5$  h rupture stress of a typical 18-12 steel, showing that the model correctly predicts best properties at a larger stabilisation ratio, although this ratio still shifts slightly towards understabilisation for longer times.

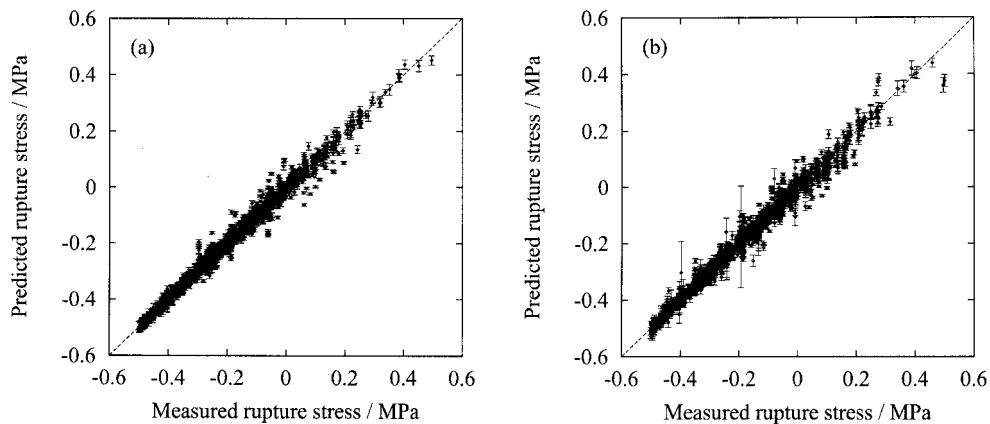
Figure 11a, shows the effect of the solution treatment temperature for different levels of Nb (see base composition in Table 2). This is in very good agreement with the hypothesis<sup>25</sup> that the optimum creep properties are obtained when as much as possible of the MX forming elements are put in solution before service: with an increased level of niobium, the solution treatment temperature that dissolves the maximum amount of Nb(C,N) is increased. Figure 11b, is a prediction of the amount of NbC (calculated with MT-DATA<sup>28</sup>) found in a steel of composition equal to that used for the predictions above, (steel with 0.32 wt-%Nb). It shows that all of the carbon and niobium are in solution only at temperatures higher than 1250°C, which closely



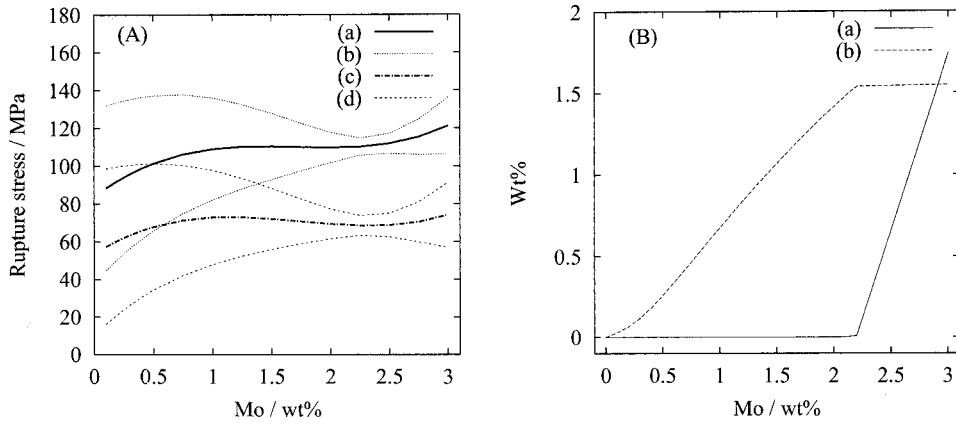
5 Perceived significances  $\sigma_w$  for first four networks, constituting the committee model for creep rupture life: S.t. solution treatment



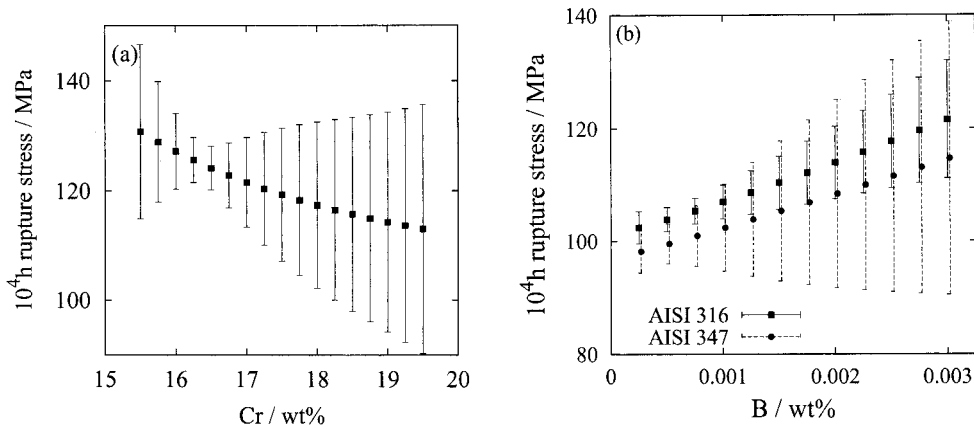
6 Performances of final committee model on whole database, for a rupture life model and b creep strength model



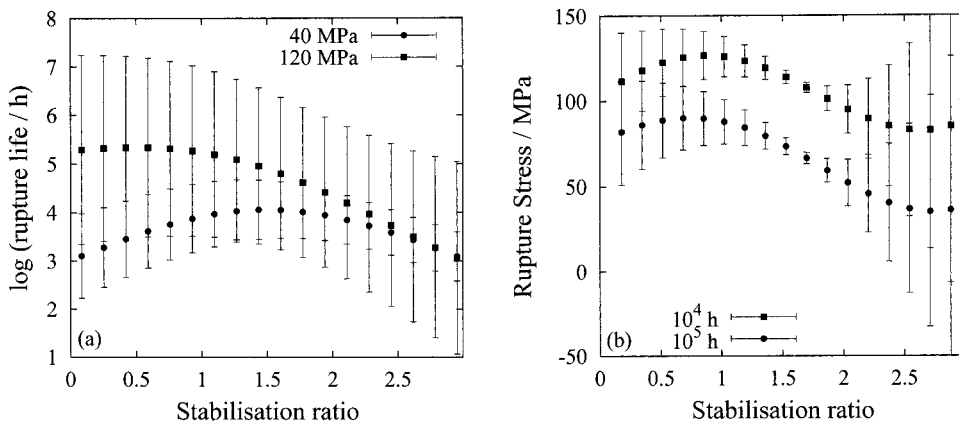
7 'Best model' prediction on training set a and test set b for creep rupture model



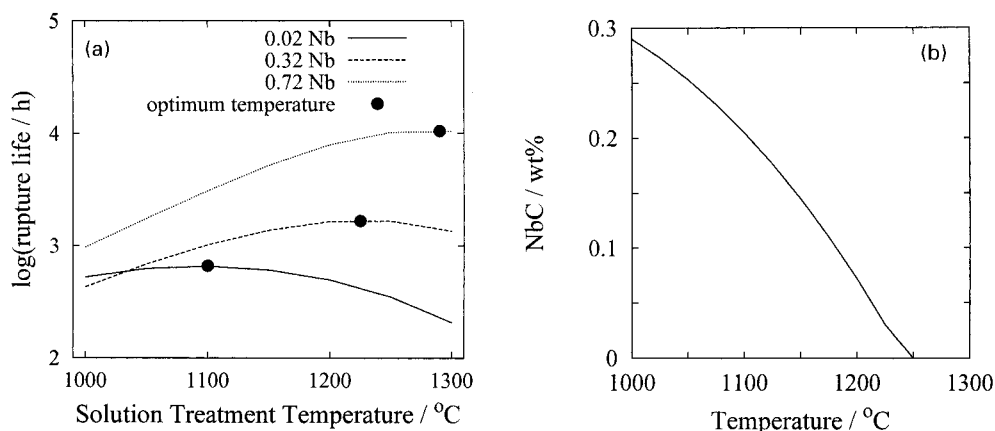
8 A the predicted effect of Mo on a  $10^4$  h and c  $10^5$  h rupture stress at  $650^\circ\text{C}$ , b and d are error bounds for a and c respectively; B MT-DATA prediction for a amount of Laves phase and b amount of Mo in solid solution in austenite for steel of same composition (phases allowed were austenite,  $\text{M}_{23}\text{C}_6$ ,  $\text{M}_6\text{C}$ , Laves phase,  $\sigma$  phase, ferrite and liquid) base composition used can be found in Table 2



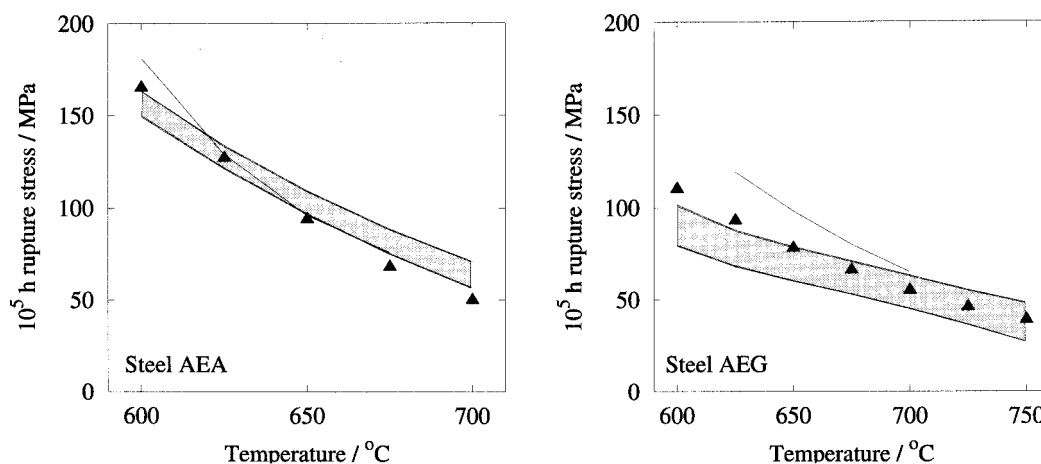
9 a predicted influence of chromium on the  $10^4$  h rupture stress at  $650^\circ\text{C}$  for typical 316 steel; b effect of boron on creep rupture stress for two different steels, 316 and 347; detailed compositions for these examples are given in Table 2



10 a effect of the stabilisation ratio (increase in Nb) on creep rupture life of typical 18Cr–12Ni steel at  $650^\circ\text{C}$ : optimum short term creep properties are obtained for close to stoichiometric additions, while understabilisation is better for long term properties; b effect of an increase in Ti: stabilisation ratio which produces the optimum creep strength is larger than in a



11 a predicted effect of solution treatment temperature on creep rupture life of typical 18–12 steel (see Table 2); b amount of NbC present as function of solution treatment temperature, in 0.32 wt-%Nb steel, calculated MT-DATA (allowing for austenite, ferrite, liquid, TiC, NbC, TiN, NbN,  $M_{23}C_6$  and  $\sigma$  phase)



12 Comparison between neural network model predictions (shaded area), predictions made by NRRM using Orr–Sherby–Dorn method (line) and experimental values published in recent revision 28B (points): see Table 2 for full compositions

matches the optimum solution treatment temperature for this composition.

## COMPARISON WITH OTHER METHODS

The recent revision of the NRRM (National Research Institute for Metals, Japan) datasheet no. 28 (28B, data for SUS 347H TB) contains considerably more long term data than did the previous version 28A. At the time when the database used in the present work was compiled, these new data were not available and therefore have not been used to train the models. It is interesting to compare the predictions of the present model with those made by the NRRM on the same data.

The  $10^5$  h rupture stress was predicted using the neural network model for two steels taken from the NRRM 28B datasheet (AEA and AEG), for temperatures ranging between 600 and 750°C.

Figure 12 shows the predictions of the neural network model against those made by the NRRM, using the Orr–Sherby–Dorn method, on the previously published data, and the recent results published in revision 28B. The agreement with experimental data is good, particularly in the case of steel AEG where the neural network gives significantly better predictions than the Orr–Sherby–Dorn method used by the NRRM. It should also be noticed that the trends for both steels have been correctly predicted, despite their apparent similarity in composition (see Table 2).

## SOFTWARE

A number of other trends predicted by the models have been examined, which have been found to be reasonable from a metallurgical point of view, among which a positive effect of Cu, of P within a limited range (however this element causes

Table 2 Base compositions of the different examples, wt-%

Fig.	Cr	Ni	Mo	Mn	Si	Nb	Ti	V	Cu	N	C	B (ppm)	P	S	Co	Al
8	18.0	12.0	...	1.4	0.6	0	0	0	0	0	0.06	5	0.02	0.01	0	0
9a	...	12.1	2.54	1.41	0.46	0	0	0	0	0	0.04	0.0002	0.019	0.02	0	0
9b, 316	16.42	13.21	2.34	1.51	0.52	0.01	0.011	0	0.14	0.034	0.05	...	0.021	0.01	0	0
9b, 347	17.89	12.55	0.11	1.74	0.77	0.77	0.02	0.033	0.09	0.016	0.05	...	0.025	0.007	0.37	0.004
10a	18.15	13.3	0	0.75	0.4	0.1	0	0	0	0.012	0.062	0	0.02	0.002	0	0
10b	17.71	12.27	0.02	1.56	0.55	0.005	...	0	0.06	0.014	0.06	5	0.026	0.01	0	0.121
11a	18	12	0.05	0.8	0.4	0.02	0.02	0	0	0.01	0.06	10	0.02	0.002	0	0
12(AEA)	17.85	12	0.04	1.71	0.60	0.74	0.019	0.031	0.05	0.0284	0.07	12	0.02	0.005	0.29	0.019
12(AEG)	17.56	12.24	0.15	1.81	0.63	0.87	0.019	0.041	0.14	0.0222	0.053	27	0.027	0.011	0.30	0.008



embrittlement and is therefore kept much below the level giving optimum creep rupture strength). The number of possibilities of interactions are such that it is not possible to study them fully. The database used to create the model covers a large range of compositions and its application does not stop at the AISI 300 series. The software capable of doing these calculations can be obtained freely from <http://www.msm.ac.uk/map/map.html>.

## Summary and conclusions

The creep rupture life for a given stress, and the creep rupture stress for a given life have been analysed using a neural networks method within a Bayesian framework. The data were obtained from a variety of sources and cover a wide range of compositions and heat treatments. The potential of the method is clearly illustrated in its ability to perceive interactions between the different input variables. Predicted trends have been found consistent with those expected and the quantitative agreement was frequently satisfying. The model can be applied widely because of its capacity to indicate uncertainty, including both an estimate of the perceived level of noise in the output, and an uncertainty associated with fitting the function in the local region of input space.

## Acknowledgements

The authors are grateful to Innogy Plc and EPSRC for funding the project of which this work is part, and to Professor D. Fray for provision of laboratory facilities.

## References

1. P. MARSHALL: 'Austenitic stainless steels, microstructure and mechanical properties'; 1984, London, Elsevier.
2. D. J. C. MACKAY: in 'Mathematical modelling of weld phenomena 3', (ed. H. Cerjak), 359–389; 1997, London, The Institute of Materials.
3. H. K. D. H. BHADESHIA: *ISIJ Int.*, 1999, **39**, 966–979.
4. D. J. C. MACKAY: *Neural Comput.*, 1992, **3**, 448–472.
5. The British Steelmakers Creep Committee: 'BSCC high temperature data'; 1973, London, The Iron and Steel Institute.
6. J. K. L. LAI: *Mater. Sci. Technol.*, 1985, **1**, 97–100.
7. Y. MINAMI, H. KIMURA, and M. TANIMURA: in 'New developments in stainless steel technology', (ed. R. Lula), 231–242; 1985, Metals Park, OH, American Society for Metals.
8. E. A. JENKINSON, M. F. DAY, A. I. SMITH, and L. M. T. HOPKIN: *J. Iron Steel Inst.*, 1962, **200**, 1011–1024.
9. D. G. MORRIS: *Metal Sci.*, 1978, **12**, 19–29.
10. V. A. BISS and V. K. SIKKA: *Metall. Trans. A*, 1981, **12A**, 1360–1362.
11. J. STRUTT and K. S. VECCHIO: *Metall. Trans. A*, 1999, **30A**, 355–362.
12. V. VORÁDEK: in 'Applications of stainless steels '92', (ed. H. Nordberg and J. Björklund), 123–132; 1992, Stockholm, Jernkontoret.
13. S. R. KEOWN and F. B. PICKERING: in 'Creep strength in steel and high-temperature alloys', 229–234; 1974, London, The Metals Society.
14. K. J. IRVINE, J. D. MURRAY, and F. B. PICKERING: *J. Iron Steel Inst.*, 1960, **196**, 166–179.
15. GITTINS: *J. Mater. Sci.*, 1970, **5**, 223–232.
16. T. TAKAHASHI, M. SAKAKIBARA, M. KIKUCHI, S. ARAKI, T. OGAWA, and K. NAGAO: in 'Improved coal-fired power plants', (ed. A. F. Armor *et al.*), Vol. 1, 3–17; 1991, Palo Alto, CA, Electric Power Research.
17. H. NAOL, M. OHGAMI, S. ARAKI, T. OGAWA, T. FUJITA, H. MIMURA, H. SAKAKIBARA, Y. SOGON, and H. SAKURAI: *Nippon Steel Tech. Rep.*, April 1993, (57), 22–27.
18. S. ARAKI, T. TAKAHASHI, M. SAKAKIBARA, H. MIMURA, T. ISHITSUKA, H. NAOL, and T. FUJITA: in 'Microstructures and mechanical properties of aging materials', (ed. P. K. Liaw), 99–105; 1992, Warrendale, PA, TMS.
19. S. ARAKI, T. TAKAHASHI, and M. SAKAKIBARA: in 'Life prediction of corrodible structures', 1–15; 1991, Houston, TX, NACE.
20. T. TAKAHASHI, M. KIKUCHI, and H. SAKURAI *et al.*: *Nippon Steel Tech. Rep.*, July, 1988, (38), 26–33.
21. M. D. MATHEW, G. SASIKALA, K. B. S. RAO, and S. LMANNAN: in 'Creep: characterization, damage, and life assessment', 5th Int. Conf. on 'Creep of materials', (ed. D. A. Woodford *et al.*), 577–585; 1992, Materials Park, OH, ASM International.
22. D. J. C. MACKAY: 'Probable networks and plausible predictions – A review of practical bayesian methods for supervised neural networks', Internet: <http://wol.ra.phy.cam.ac.uk/mackay/BayesNets.html>, 1995.
23. D. ELLIOTT and S. M. TUPHOLME: 'An introduction to steel selection: Part 2, Stainless steels' 1981, Oxford, Oxford University Press.
24. F. B. PICKERING: 'Physical metallurgy and the design of steels'; 1978, London, Applied Science Publishers.
25. M. KIKUCHI, M. SAKABIBARA, Y. OTOGURO, M. MIMURA, T. TAKAHASHI, and T. FUJITA: in 'International conference on creep', Tokyo, Japan, April 1986, 215–220.
26. T. SOURMAIL: *Mater. Sci. Technol.*, 2001, **17**, 1–14.
27. F. MASUYAMA: in 'Advanced heat resistant steels for power generation', (ed. R. Viswanathan and R. Nutting), 33–47; 1998, London, The Institute of Materials.
28. 'MT-DATA handbook: utility module'; Teddington, Middx, National Physical Laboratory.